RESEARCH REVIEW JOURNALS
Volume-04
Issue-12
December -2019

ISSN: 2455-3085 (Online)
RESEARCH REVIEW International Journal of Multidisciplinary
www.rrjournals.com[Peer Reviewed Journal]

Finite Element based thermal analysis of a rotary Kiln seal

[1]K. Saminathan & [2]Madhanagopal Krishnan

[1]*FEA specialist, Group Engineering, FLSmidth, Chennai (India)*
[2]*Development specialist, Group Engineering, FLSmidth, Chennai (India)*

ARTICLE DETAILS

Article History
Published Online: 16 Dec 2019

Keywords
Rotary kiln, lamella kiln seal, thermal contact conductance, infra-red thermometer, kiln shell, steady-state thermal analysis

***Corresponding Author**
Email: ksaminathan25[at]gmail.com

ABSTRACT

Lamella type seals are widely used in rotary kilns for sealing the connection between a rotating kiln and the stationary parts. In the present research work, a finite element based methodology is developed to predict the temperature distribution across a rotary kiln seal installed in a cement plant. Loads and boundary conditions are arrived based on literature and the plant data. Experimental measurement of temperature on the parts of kiln seal has been carried out using a non-contact type infra-red thermometer. A steady-state thermal analysis has been performed to predict the temperature on the kiln seal. It is found the Finite Element results are in good agreement with experimental results.

1. Introduction

A rotary kiln is a pyro-processing device that raises materials to a very high temperature in a continuous process. It can be divided into cement rotary kiln, metallurgy rotary kiln and lime rotary kiln. Cement rotary kiln is mainly used to calcine cement clinker, and the Metallurgy kiln is used to calcine lean iron ore, bauxite, aluminum hydroxide, chrome ore etc. Lime rotary kiln is used to calcine active lime and light roasting dolomite.

Rotary kiln is typically in a cylindrical shape and made of steel plate, inside of which a refractory lining is placed. Rotary kilns are normally kept at an inclination to make the gravity to aid the material movement from one side to other. Tiers support the kiln at two or three locations. The kiln is rotated by a ring gear arrangement which is driven by a motor through a gear box system to get the required speed reduction. A typical rotary kiln system is shown in figure 1.

The kiln is rotated around its axis (one end is usually slightly higher than the other). The material is entered one side of the kiln (the higher end) and as the rotation occurs, the material slides down through the tube and goes through a certain amount of mixing and stirring. Heat is normally supplied at the other end from an external source called burner. Heat and feed is flowing in opposite directions within the kiln shell so that the feed is constantly increasing in temperature from start to finish. After the sintering process, the material is calcined into cement clinker and discharged into cooler machine through kiln hood

Kiln seals are used to connect the rotating kiln with the stationary parts on either side. Here, the kiln seal serves the purpose of sealing the domain where the rotating kiln enter a stationary kiln head hood. A seal is essential at each end of a rotary unit to prevent ambient air from entering the process. Air leakage can have varying effects on different processes and a leaky seal may reduce efficiency, create unsafe or unstable conditions.

Lamella type seals are frequently used in rotary cement kilns. A typical lamella kiln seal arrangement is shown in figure 2. It connects the rotating kiln with the stationary kiln hood. The kiln shell, outlet sector and the Cooling jacket with the drive link are the rotating members. The kiln hood, dust chamber and lamella are the stationary members. The lamella sits on a wear tire which is rigidly fixed with the cooling jacket.

The outer surfaces of the kiln hood, the dust chamber, the lamella and a smaller end portion of the cooling jacket are exposed to ambient air. A forced air cooling, driven by a series of fans, is applied on the space between the kiln shell and the cooling jacket.

During operation, kiln seal components are exposed to a high temperature. Phenomenon such as creep, oxidation and wear are dominant at high temperature, and they lead to material degradation. A High temperature gradient and a larger variation in the co-efficient of thermal expansion of adjacent components lead to severe thermal distortion and eventually a failure. A proper design of these components requires a complete temperature distribution across the kiln seal.

Nowadays, Finite Element based analysis is widely used to find the temperature distribution in industrial components. Gonfa et al [2] developed a 3-dimensional finite element based model and studied the heat transfer process in a rotary kiln. Jagendran et al [3] used a Finite element based thermal analysis to determine the optimum coating thickness for good insulation and durability of the kiln. Susana et al [4] developed a finite element model of a cement rotating kiln to predict the temperature inside the kiln/refractory. Jia et al [5] developed a finite element based model for lime rotary kilns, to study the structural and thermal distribution, which helped in the optimization of the kiln cylinder. In most of the researches, the FE analyses are focused on rotary kiln, not on the kiln seal. A finite element based methodology to predict the temperature distribution across a rotary kiln seal assembly is rarely reported in the literature, and it is proposed in the present research work

The objective of the present work is to develop a finite element methodology to predict the temperature distribution across a rotary kiln seal and validate through experimental results.

For the present research work, the lamella kiln seal of rotary kiln at line one of Chettinad Cement Corporation Private Limited, Ariyalur, Tamilnadu, India, has taken up for the Finite element study and experimental investigations.

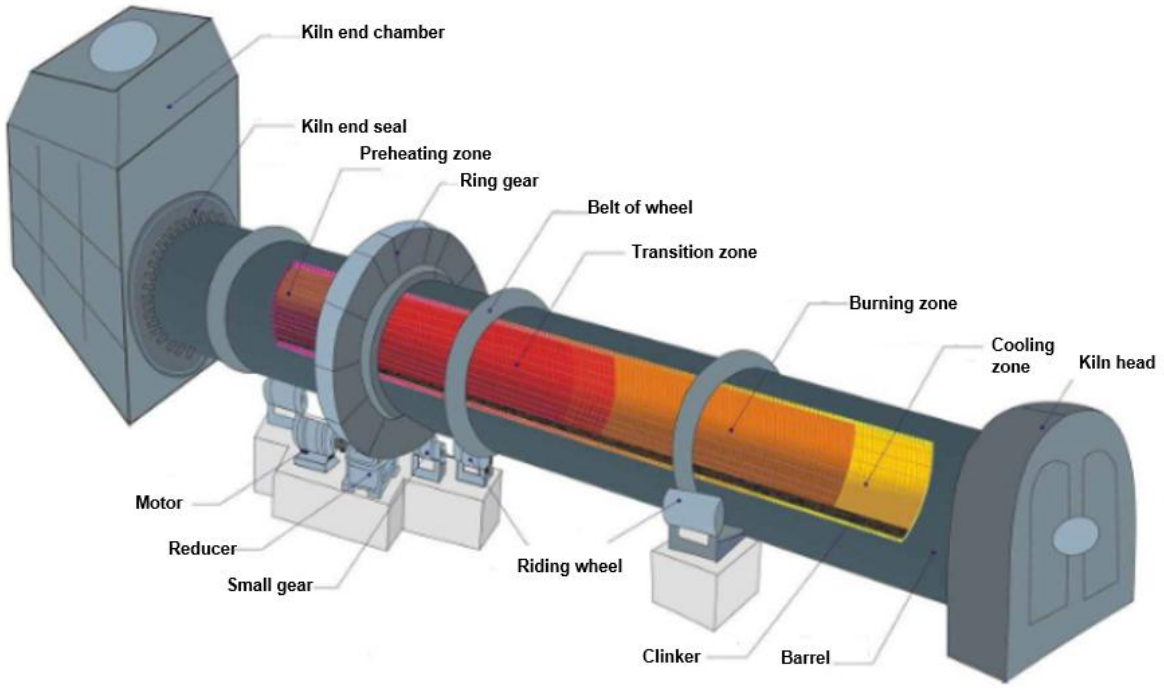

Figure 1. Arrangement of rotary kiln

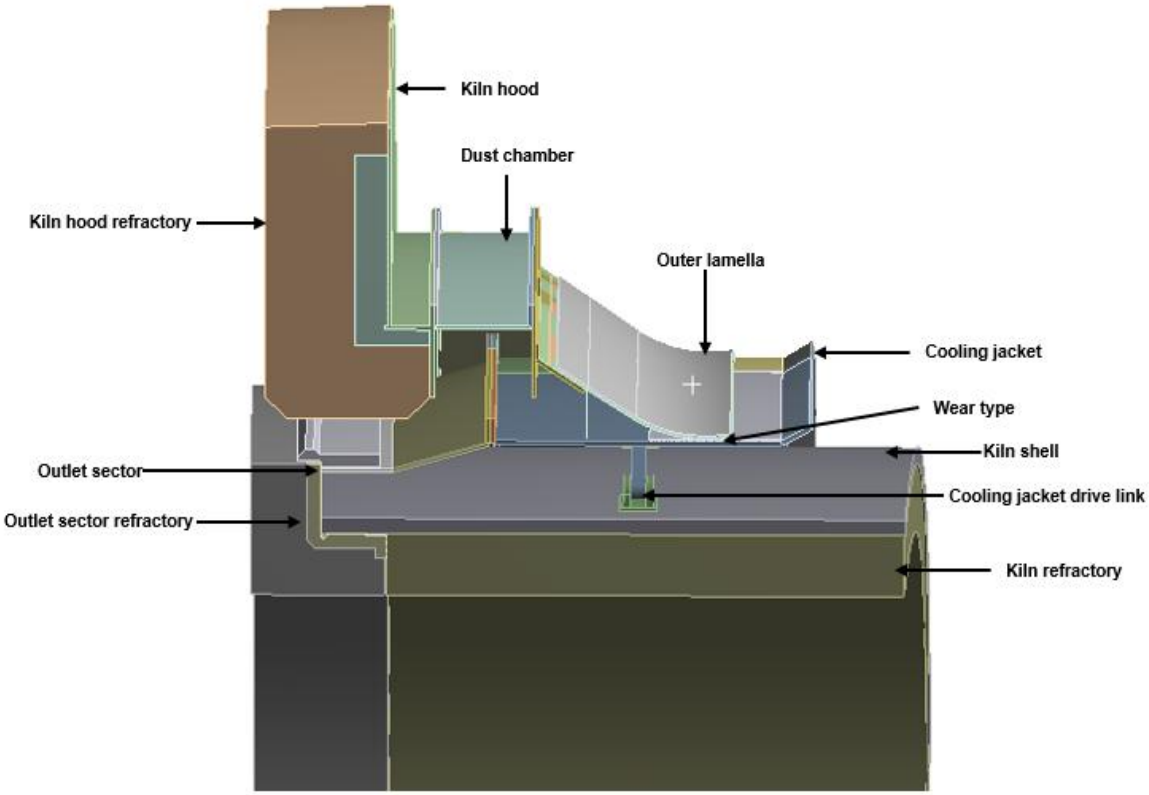

Figure 2. Parts of a rotary kiln seal

2. Governing equations

The basic equation of heat transfer has the following form

$$-\left(\frac{\partial q_x}{\partial x}+\frac{\partial q_y}{\partial y}+\frac{\partial q_z}{\partial z}\right)+Q=\rho c\frac{\partial T}{\partial t} \quad \text{..... (1)}$$

Here, q_x, q_y and q_z are the components of heat transfer through unit area, Q=Q (x, y, z, t) is the inner heat generation rate per unit volume; **ρ** is the material density; c is heat capacity; T is temperature and 't' is time

According to Fourier's law, the components of heat flow can be expressed as below

$$q_x=-k\frac{\partial T}{\partial x} \quad \text{..... (2)}$$

$$q_y=-k\frac{\partial T}{\partial y} \quad \text{..... (3)}$$

$$q_z=-k\frac{\partial T}{\partial z} \quad \text{..... (4)}$$

k is thermal conductivity of the media, substitution of Fourier's relations in equation (1) gives the following heat transfer equation

$$\frac{\partial}{\partial x}\left(k\frac{\partial T}{\partial x}\right)+\frac{\partial}{\partial y}\left(k\frac{\partial T}{\partial y}\right)+\frac{\partial}{\partial z}\left(k\frac{\partial T}{\partial z}\right)+Q=\rho c\frac{\partial T}{\partial t} \quad \ldots (5)$$

It is assumed that the boundary conditions can be of the following types

Specified temperature

$T_s=T1(x, y, z, t)$ on S_1 …… (6)

Specified heat flow

$q_xn_x+q_yn_y+q_zn_z=-q_s$ on S_2 … (7)

Convection boundary conditions

$q_xn_x+q_yn_y+q_zn_z=h(T_s-T_e)$ on S_3 ... (8)

Radiation boundary conditions

$q_xn_x+q_yn_y+q_zn_z=\sigma\varepsilon T_s^4-\alpha q_r$ on S_4 … (9)

where *h* is the convection coefficient; T_s is an unknown surface temperature; T_e is a convective exchange Temperature; σ is the Stefan–Boltzmann constant; ε is the surface emission coefficient; α is the surface absorption coefficient, and q_r is the incident radiant heat flow per unit surface area. S_1, S_2, S_3, and S_4 are surfaces on which thermal boundary conditions are specified

For transient problems it is necessary to specify an initial temperature field for a body at the time $t = 0$: $T(x, y, z, 0) = T_0(x, y, z)$.

In a Finite Element calculation, a domain 'V' is divided into finite elements connected at nodes, and all the relations are written for a finite element. Global equations for the domain can be arrived by assembling the finite element equations using connectivity information.

Shape functions Ni are used for the interpolations of temperature inside a finite element

$$T=[N]\{T\} \quad \ldots.. (10)$$

$$[N]=[N1\ N2\ \ldots] \quad \ldots.. (11)$$

$$\{T\}=\{T1\ T2\ \ldots.\} \quad \ldots.. (12)$$

Differentiation of temperature-interpolation equation gives the following interpolation relation for the temperature gradients

$$\begin{Bmatrix}\frac{\partial T}{\partial x}\\ \frac{\partial T}{\partial y}\\ \frac{\partial T}{\partial z}\end{Bmatrix}=\begin{bmatrix}\frac{\partial N_1}{\partial x} & \frac{\partial N_2}{\partial x} & \ldots\\ \frac{\partial N_1}{\partial y} & \frac{\partial N_2}{\partial y} & \ldots\\ \frac{\partial N_1}{\partial z} & \frac{\partial N_2}{\partial z} & \ldots\end{bmatrix}\{T\}=[B]\{T\} \quad \ldots (13)$$

Here, {T} is a vector of temperatures at nodes, [*N*] is a matrix of shape functions, and [*B*] is a matrix for temperature-gradient interpolation.

Using the Galerkin method, the basic heat transfer equation (5) can be written in the following form:

$$\int_V\left(\frac{\partial q_x}{\partial x}+\frac{\partial q_x}{\partial x}+\frac{\partial q_x}{\partial x}-Q+\rho c\frac{\partial T}{\partial t}\right)N_i\,dV=0 \quad \ldots. (14)$$

Applying divergence theorem to the first three terms of equation (14), the following relations are arrived

$$\int_V\rho c\frac{\partial T}{\partial t}N_i\,dV-\int_V\left[\frac{\partial N_i}{\partial x}\ \frac{\partial N_i}{\partial y}\ \frac{\partial N_i}{\partial z}\right]\{q\}\,dV=\int_V QN_i\,dV-\int_{S1}\{q\}^T\{n\}N_i\,dS \quad \ldots. (15)$$

$$\{q\}^T=\begin{bmatrix}q_x\ q_y\ q_z\end{bmatrix} \quad \ldots. (16)$$

$$\{n\}^T=\begin{bmatrix}n_x\ n_y\ n_z\end{bmatrix} \quad \ldots (17)$$

where {n} is an outer normal to the surface of the body. After insertion of boundary conditions into the above equation, the discretized equations are as follows

$$\int_V\rho c\frac{\partial T}{\partial t}N_i\,dV-\int_V\left[\frac{\partial N_i}{\partial x}\ \frac{\partial N_i}{\partial y}\ \frac{\partial N_i}{\partial z}\right]\{q\}\,dV=\int_V QN_i\,dV-\int_{S1}\{q\}^T\{n\}N_i\,dS+\int_{S2}q_s\,N_i\,dS+\int_{S3}h(T-T_e)N_i\,dS+\int_{S4}(\sigma\varepsilon T^4-\alpha q_r)N_i\,dS \quad \ldots (18)$$

$$\{q\}=-k\,[B]\{T\} \quad \ldots. (19)$$

The discretized finite element equations for heat transfer problems have the following form:

$$[C]\{\dot{T}\}+([K_c]+[K_h]+[K_r])\{T\}=\{R_T\}+\{R_Q\}+\{R_q\}+\{R_h\}+\{R_r\} \quad \ldots. (20)$$

Where,

$$[C]=\int_V\rho c[N]^T[N]dV \quad \ldots (21)$$

$$[K_c]=\int_V k[B]^T[B]\,dV \quad \ldots (22)$$

$$[K_h]=\int_{S3}h\,[N]^T[N]\,dS \quad \ldots (23)$$

$$[K_r]\{T\}=\int_{S4}\sigma\varepsilon T^4[N]^T\,dS \quad \ldots (24)$$

$$[R_T]=-\int_{S1}\{q\}^T\{n\}\,[N]^T dS \quad \ldots (25)$$

$$[R_Q]=\int_V Q[N]^T dV \quad \ldots (26)$$

$$[R_q]=\int_{S2}q_s\,[N]^T dS \quad \ldots (27)$$

$$[R_h]=\int_{S3}hT_e[N]^T dS \quad \ldots (28)$$

$$[R_r]=\int_{S4}\alpha\,q_r[N]^T dS \quad \ldots (29)$$

Here, $\{\dot{T}\}$ is a nodal vector of temperature derivatives with respect to time

In the present study, it is expected that the temperature distribution across the kiln seal should be below 400^0 C, as the kiln shell temperature is around 350^0 C based on the CCR (Central Control Room) data available at site. At this temperature, heat transfer through radiation may be small and is neglected in the present calculation.

For a non-linear steady state problem with no radiation, the above equation (20) reduces to

$$([K_c]+[K_h])\{T\}=\{R_Q(T)\}+\{R_q(T)\}+\{R_h(T)\} \quad \ldots (30)$$

In the Finite Element based thermal analysis of rotary kiln seal, the above equation (30) is solved to establish the temperature distribution across the components of the kiln seal.

3. FE Model setup

3.1 Model discretization

The CAD model of the kiln seal is made using SOLIDWORKS CAD software, and it is imported into ANSYS design modeler application. The imported CAD model is simplified by removing intricate details, which do not affect much the heat transfer between the parts. The CAD model simplification is performed for a better discretization of the domain. The geometrical arrangement of parts, the loads and the boundary conditions offer a half symmetry -reduced model approach for Finite Element calculations. This reduced model approach will drastically reduce the solution time without compromising the accuracy of the results. A half symmetry model is created from the simplified CAD model.

The half symmetry model is imported into ANSYS mechanical meshing application and discretized into finite elements using hex dominant meshing algorithm. The discretized model has ANSYS elements SOLID 87, SOLID 90 and SHELL 131, and the total number of elements is 844,844 with 2,424,636 nodes. The global aspect ratio of the FE model is 1.83.

3.2 Contact definition

Bonded contacts used in ANSYS mechanical application, are defined between the parts of the kiln seal which are in physical contact. In this type of contact, a perfect thermal contact conductance is assumed, meaning that no temperature drop occurs at the interface.

Numerous conditions like surface flatness, surface finish, oxides, entrapped fluids and use of conductive grease can contribute to less than a perfect contact conductance. But, these effects are not considered in the finite element calculations.

The amount of heat flow across a contact interface is defined by the contact flux q.

$$q = TCC(T_{target} - T_{contact})$$

TCC (Thermal Contact Conductance) is set to a relatively high value based on the largest thermal conductivity defined in the model, k, and the diagonal of the overall geometry bounding box.

$$TCC = k.\frac{10000}{diagonal\ of\ bounding\ box}$$

This essentially provides a perfect conductance between the parts and results a minimum drop in temperature across the interface.

3.3 Material definition

Table 1 shows the different parts of the kiln seal along with their material of construction. Figure 3 to figure 14 shows their temperature dependent thermal conductivity. The material properties are arrived from an internal FLSmidth material library.

All the materials are created with appropriate temperature dependent material properties in 'Engineering Data' cell of a Steady-State Thermal analysis system in ANSYS workbench application. In the Finite Element model, all the components of the kiln seal are assigned with the respective material type.

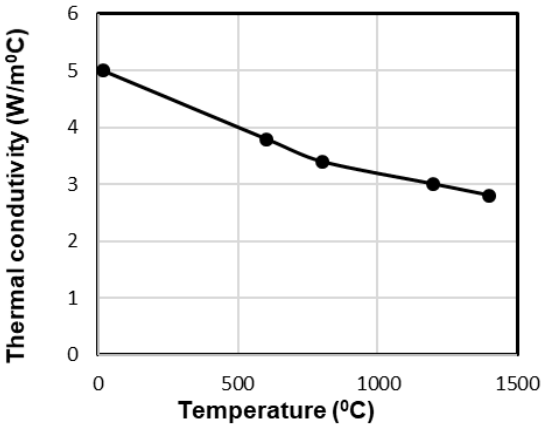

Figure 3. BA10 – Temperature Vs. thermal conductivity

Table 1
Materials for kiln seal components

Sl.no.	Part's name	Assigned Material
1	Kiln Refractory	BA-10 (block insulation)
2	Kiln shell	Carbon steel
3	Outlet sector	Heat resistant cast steel
4	Outlet sector flange/shim	Heat resistant cast steel
5	outlet sector refractory	HY-1 (hydraulic casting)
6	cooling jacket (inner casing)	Wrought stainless steel
7	cooling jacket (outer casing)	structural steel
8	wear tyre	Abrasion heat resistant steel
9	Inner and outer lamella	Spring steel
10	Heat resistant clothe and curtain	kerlane
11	dust chamber	structural steel
12	Kiln hood	structural steel
13	kiln hood insulation	IA-1/block insulation
14	Kiln hood refractory	HY-3 (hydraulic casting)

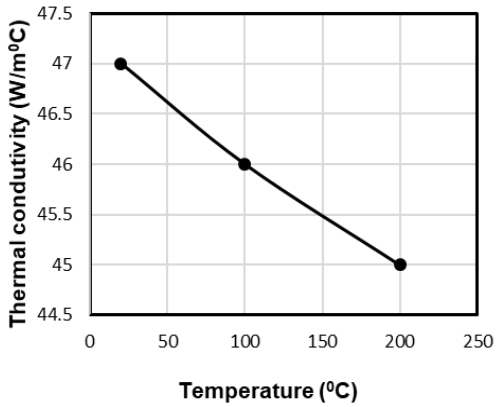

Figure 4. Abrasion heat resistant steel – Temperature Vs. thermal conductivity

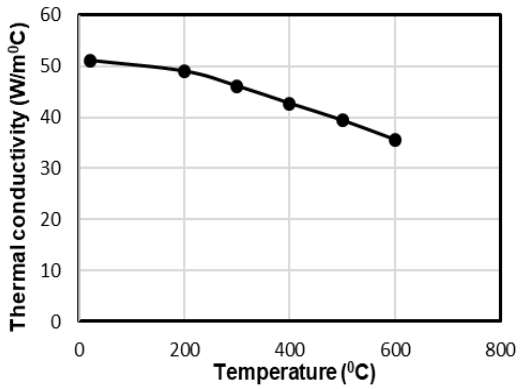

Figure 5. Carbon steel -Temperature Vs. Thermal conductivity

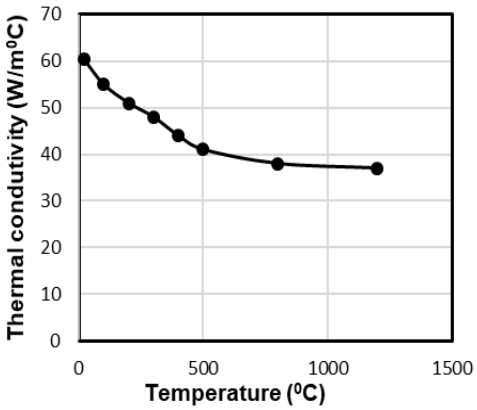

Figure 6. Carbon steel – Temperature Vs. Thermal conductivity

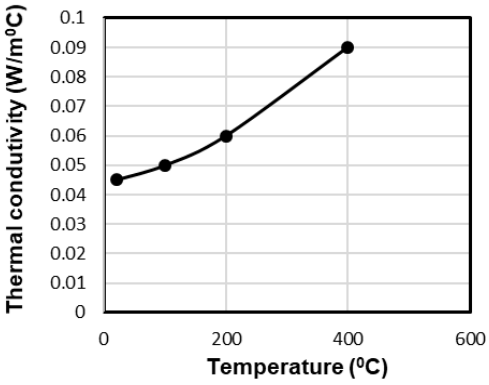

Figure 7. Heat resistant cloth – Temperature Vs. Thermal conductivity

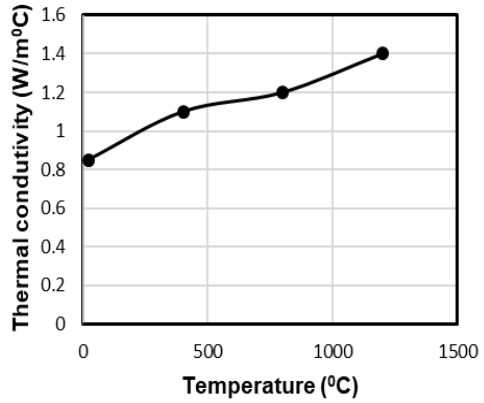

Figure 8. HY-3 (hydraulic casting) – Temperature Vs. Thermal conductivity

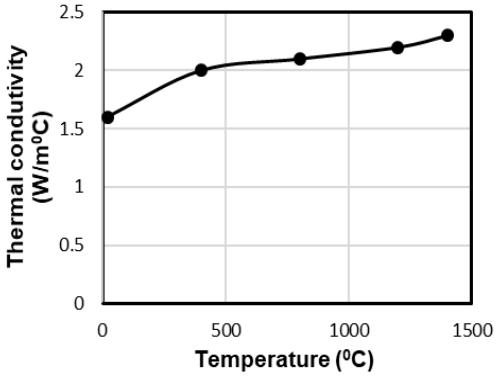

Figure 9. HY -1 (hydraulic casting) – Temperature Vs. Thermal conductivity

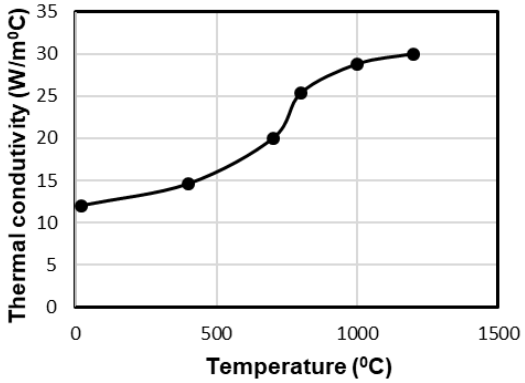

Figure 10. Heat resistant cast steel -Temperature Vs. Thermal conductivity

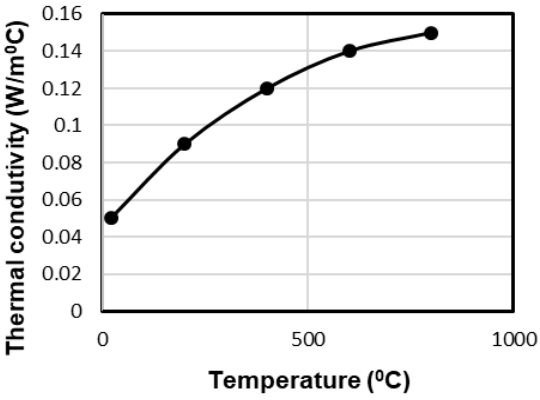

Figure 11. IA 1 (block insulation) – Temperature Vs. Thermal conductivity

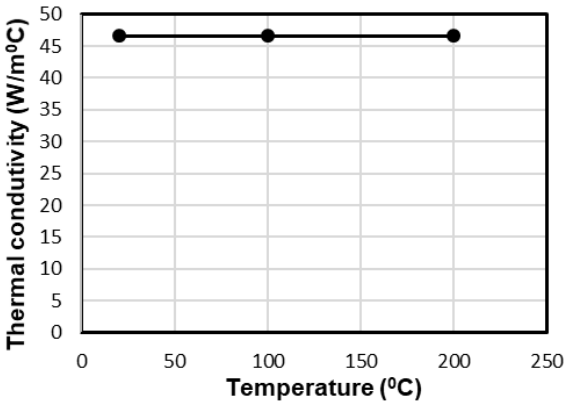

Figure 12. Spring steel – Temperature Vs. thermal conductivity

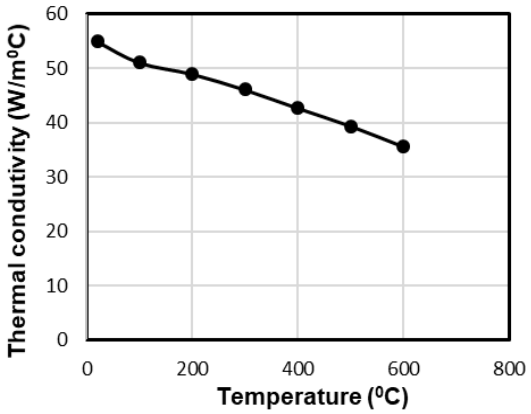

Figure 13. structural steel – Temperature Vs. Thermal conductivity

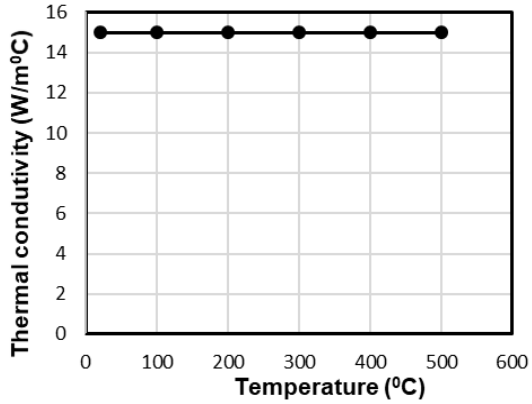

Figure 14. Stainless steel – Temperature Vs. Thermal conductivity

4. Loads and boundary conditions

In this section, thermal loads and boundary conditions used in the analysis are discussed in detail. Temperature at the inner face of kiln refractory, kiln hood refractory and outlet sector refractory are extracted from the plant data at control room. And, they are given as follow, temperature at the kiln refractory is 1100^0c and it is 1000^0c at kiln hood and outlet sector refractory.

Convective heat transfer boundary conditions are defined on three domains. Domain one consists of the outer surfaces of kiln hood, dust chamber, outer lamella and cooling jacket. Domain two comprises the inner surfaces of the dust chamber, inner lamella and a portion of outer surfaces of cooling jacket. Domain three comprises the outer surfaces of the kiln shell, elements of drive links and inner surfaces of cooling jacket.

A natural convection with a heat transfer coefficient of 15 $W/m^2\ ^0C$ is assumed for domain one as it is exposed to ambient air at a temperature of 30^0C. In domain two, surfaces are exposed to a hot air at a temperature of 400^0C, and the flow condition is similar to that of domain one as there is no forced air flow. The above facts lead to the assumption of a same heat transfer co-efficient as with domain one.

Domain three is exposed to forced air convection, as it is cooled by the flow air from a series of fans placed on either side of the rotary kiln. The calculation of heat transfer co-efficient for domain three is as below

Temperature of air from the duct $T_{hotair}=20^0$C

Temperature of the cooling jacket, $T_{tts} = 200^0$C

Average Temperature

$$T_{bulk1} = \frac{T_{hotair}+T_{tts}}{2} = 383.15\ K$$

kinematic viscosity of cooling air at T_{bulk1},

$\nu_{bulk1} = 25.91X10^{-2}$ stokes

Thermal conductivity of air at T_{bulk1}, K_{bulk1} =0.033 W/mK

Prandtl number of air at T_{bulk1}, $Pr_{bulk1} = 0.7$

Velocity of the flow V_{top}= 17 m/s

Flow length L_{top}, = 3m

Reynold's number of the flow

$$Re_{top} = V_{top}.\frac{L_{top}}{\nu_{bulk1}} \qquad \ldots\ldots (31)$$

$Re_{top} = 2.896X106$

Nusselt's number, Nu_{top} =

$$0.037\,Re_{top}^{0.8}\,\frac{Pr_{bulk1}}{(1+2.44\,Re_{top}^{-0.1\left(Pr_{bulk1}^{\frac{2}{3}}-1\right)})} \qquad \ldots\ldots (32)$$

Heat transfer coefficient at top, h_{top}

$$= Nu_{top}\frac{K_{bulk1}}{L_{top}} = 35.18\ kg/s^3K$$

So, a heat transfer co-efficient of 35 $W/m^2\ ^0C$ is considered for the surfaces on domain three.

The thermal loads and the boundary conditions. Which are applied in the FE model are shown in figure 15

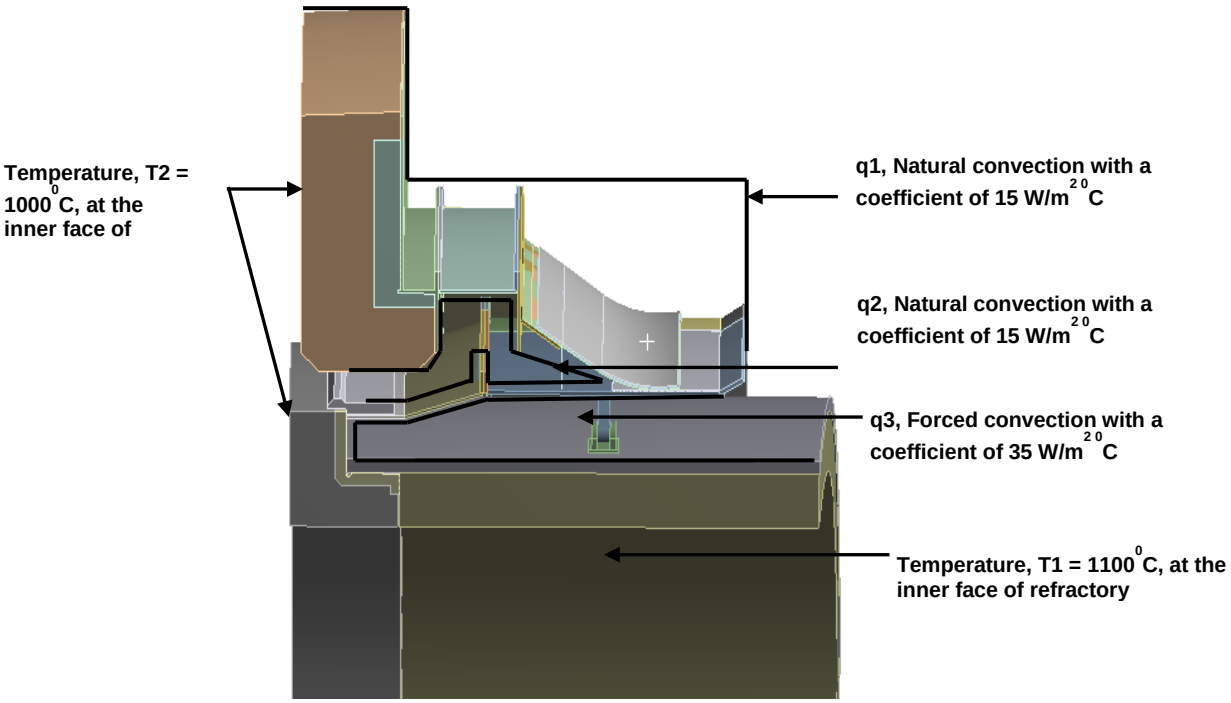

Figure 15. Thermal loads and boundary conditions

5. Experimental set up

In this section, it is explained how the temperature of each part in the kiln seal is being measured. Kiln end seal comprises both moving and stationary parts where the temperature likely to vary between 500 to 200^{0}C. Larger size of the kiln seal, surrounding high temperature parts such as kiln, and the presence of moving parts make it difficult to use the conventional temperature measuring instruments like thermocouples and other probe like sensors in this application. Hence, a non-contact type Infra-red thermometer is used to measure the temperature.

An infrared thermometer consists of a lens to focus the infra-red thermal radiation into to a detector, which converts the radiant energy into an electrical signal that can be displayed in units of temperature after being compensated for ambient temperature variations.

A MT-12 infrared thermometer is used for the temperature measurement. A temperature range of 300c to 1200^{0}c can be measured using this instrument with an accuracy of ± 2 to 3 per cent of the reading. The infrared thermometer used for this application is shown in figure.16

Figure 16. MT-12 infrared thermometer

The rotary kiln was rotating at a speed of 3 rpm. Temperature on the parts of the kiln seal was measured using the thermometer. Temperature measurement was carried out at six locations namely A, B, C, D, E and F. Locations A, B, E and F fall on kiln hood, dust chamber, cooling jacket and kiln shell respectively. Locations C and D fall on the outer lamella. The locations of temperature measurement are shown in figure 17. Five readings were measured on each location, and the average of them are presented in table 2.

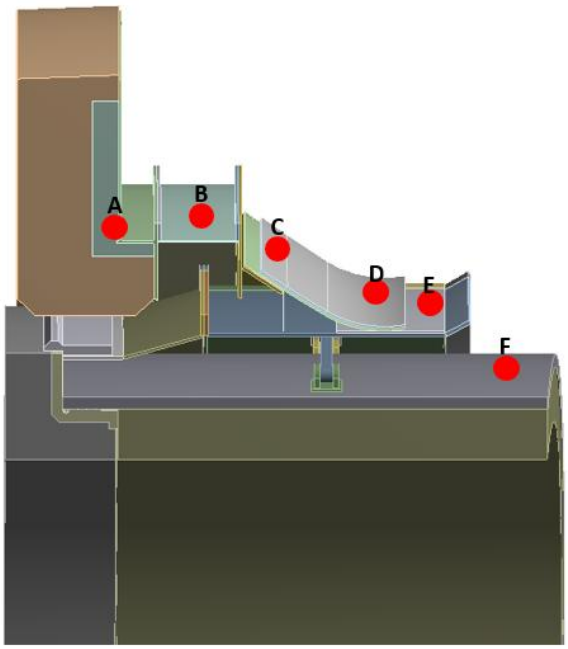

Figure 17. Locations of temperature measurement

Table 2
Temperature values at kiln seal

Sl.no.	Part's name	Temperature (^{0}C)
1	A (Kiln hood)	105

2	B (Dust chamber)	191
3	C (Outer lamella)	162
4	D (Outer lamella)	77
5	E (Cooling jacket)	70
6	F (Kiln shell)	351

6. Results and discussions

In Finite Element analysis, it is important to remove the dependency of results on the mesh density to make them more accurate. To achieve this, a four different FE model of the system are made with mesh density of 0.8, 1.2, 1.8 and 2.4 million nodes respectively.

A steady state thermal analyses are performed with the above prescribed loads and boundary conditions. FE results such as temperature on the dust chamber and cooling jacket is post processed and they are compared among all the models. It shows that FE results vary in the range of 4 to 6 per cent up to a mesh density of 1.8 million nodes. The FE results shows a variation, less than 2 per cent between the 1.8 and 2.4 million node models. Hence, a 2.4 million node FE model is selected for further investigation.

A steady state thermal analysis was performed with ANSYS WORKBENCH 19.2 on the 2.8 million nodded kiln seal FE model with the loads and the boundary conditions as discussed in section 4. The analysis has been run until the required heat convergence was obtained. The rate of heat transfer through the system was calculated using the reaction probe available with ANSYS mechanical pre-post application.

The results are presented in table 3. A positive value of heat transfer rate indicates that the heat is flowing into the system, whereas the negative sign is for the heat flowing out of the system. From the results, it is learned that the heat is flowing out of the system at outer surfaces, cooling jacket and the driving

Table 3
Heat transfer rate from FE results

Sl.no.	Part's name	Heat transfer rate (W)
1	Kiln Refractory	146980
2	Kiln hood refractory	104940
3	Outer Surfaces	-67141
4	Cooling air jacket	-237840
5	Dust chamber	55719
6	Driving elements of cooling air jacket	-2589
	Net heat transfer rate into the system	307639 W
	Net heat transfer rate out of the system	-307570 W
	Per cent of imbalance	0.022

elements of dust chamber. The heat is flowing into the system at kiln refractory, kiln hood refractory and the dust chamber. The net heat transfer rate to and out of the system are in complete balance and the amount of unbalanced heat transfer rate is 0.022 per cent and it is considered as acceptable. Hence, the FE model ensures a good heat transfer across all the parts of the system.

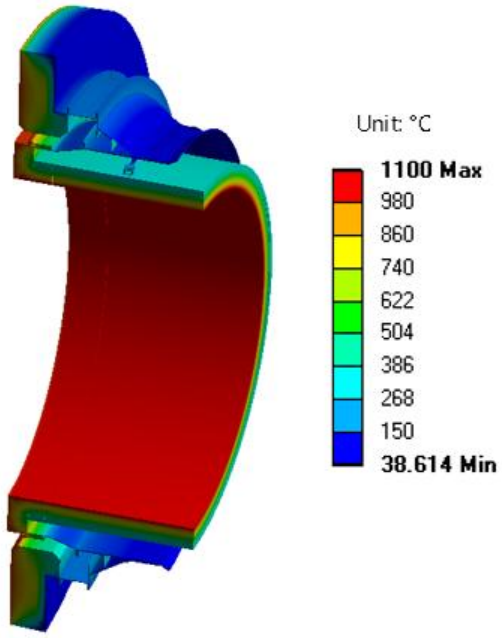

Figure 18. Temperature distribution at the kiln seal

The figure 18 shows the temperature distribution at the components of the kiln seal. The temperature varies from 39^0C to 1100^0C.

To validate the FE model of the kiln seal, temperature values are extracted from the FE result file at locations A, B, C, D, E and F, and they are compared with the experimental results. Temperature values extracted from the FE result file at the probe locations are shown in figure 19. The finite element results are closely match with the experimental results. The amount of deviation is within +- 5 per cent. Hence, the proposed finite element methodology closely predicts the temperature distribution in the kiln seal components.

The temperature distribution at the kiln shell, cooling jacket, kiln hood, dust chamber, outlet sector and outlet sector flange are shown in figure 20, figure 21, figure 22, figure 23, figure 24 and figure 25 respectively.

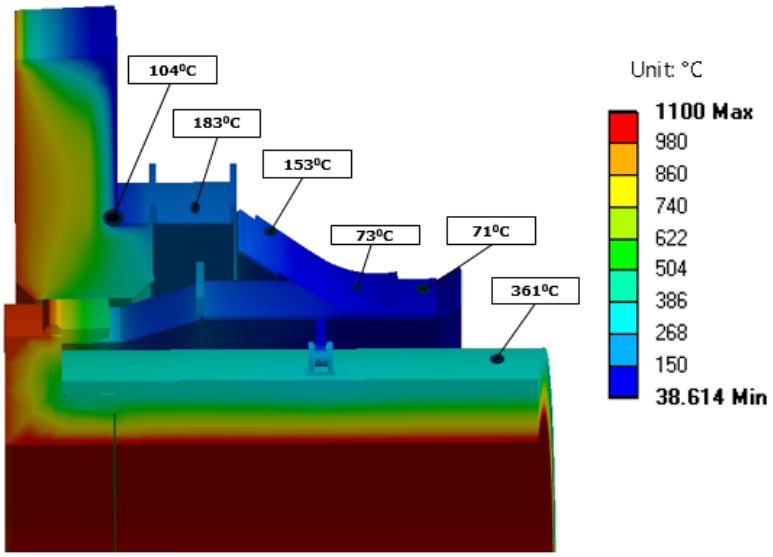

Figure 19. Temperature values at the inspection points

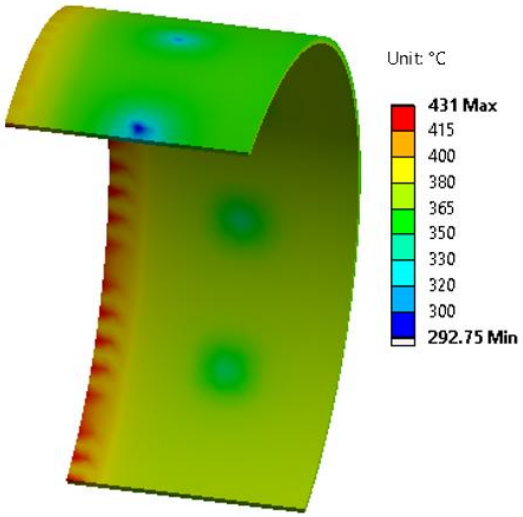

Figure 20. Temperature distribution at kiln shell

Temperature distribution at the kiln shell, cooling jacket, kiln hood, dust chamber, outlet sector and outlet sector flange is in the range of 293^{0}C- 430^{0}C, 48^{0}C-785^{0}C, 56^{0}C – 325^{0}C, 170^{0}C-222^{0}C, 403^{0}C-1000^{0}C and 452^{0}C- 1000^{0}C respectively.

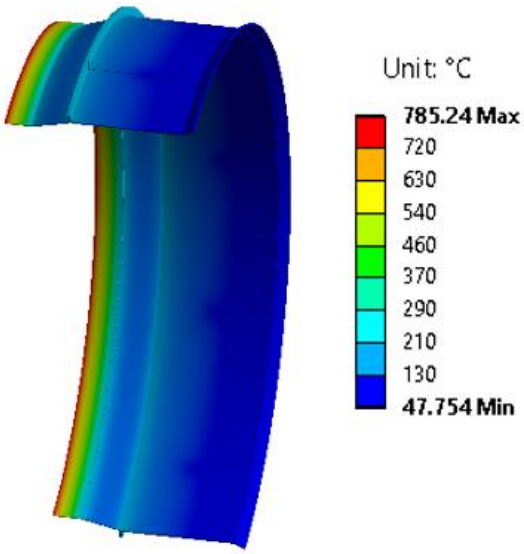

Figure 21. Temperature distribution at cooling jacket

Figure 22. Temperature distribution at kiln hood

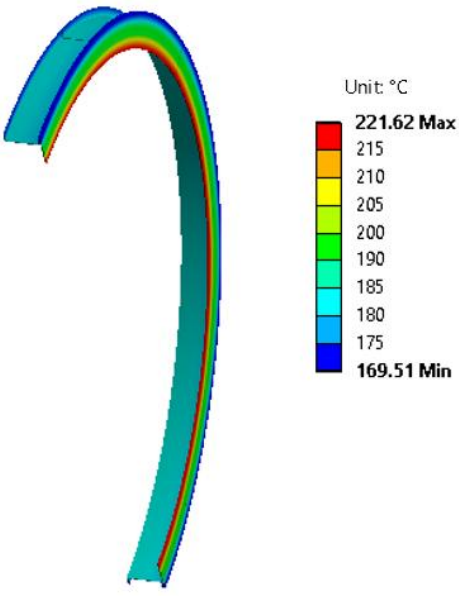

Figure 23. Temperature distribution at dust chamber

Temperature distribution on the individual parts of the kiln seal plays in a vital role in the design and selection of materials. The information of temperature distribution on the individual components of lamella kiln seal can be used to judge their performance during operation.

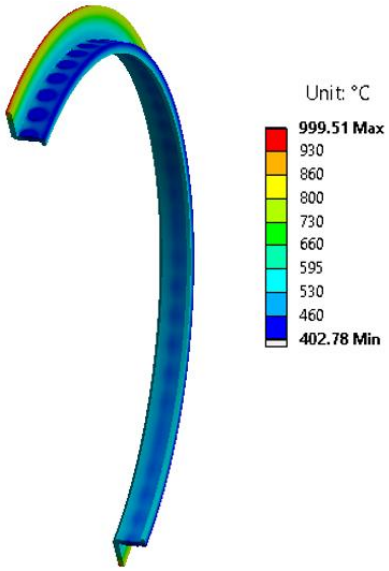

Figure 24. Temperature distribution at outlet sector

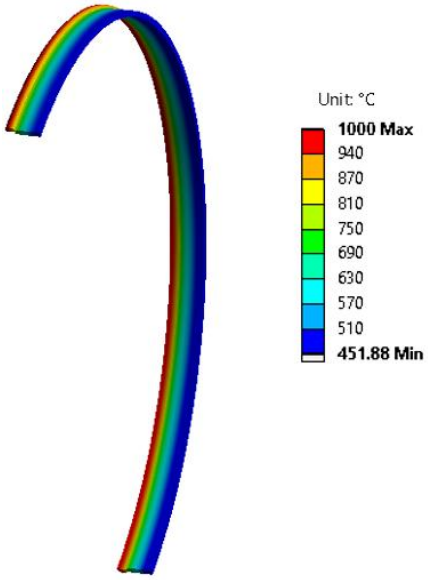

Figure 25. Temperature distribution at outlet sector flange

As the proposed finite element based methodology accurately predicts the temperature distribution across the components of the kiln seal. The same thermal loads can be used to predict the stress level on individual components using a coupled thermal-structural analysis.

7. Conclusions

In the present research work, a Finite Element based methodology is demonstrated to predict the temperature distribution at the components of a lamella type kiln seal used in a cement plant. A half symmetry model is used in the analysis to reduce the analysis time. Temperature dependent material properties are used in the analysis. Natural Convective heat transfer co-efficient values are taken from literature and forced air convective heat transfer co-efficient values are derived using appropriate relations. The Finite Element model is refined enough to make the results independent of mesh density. Temperature measurement on the kiln seal components has been carried out using a non-contact type infra-red thermometer. The FE results are in good agreement experimental results. So, the proposed Finite Element methodology can be used to predict the temperature distribution on lamella type seals used in rotary kiln.

References

1. J.J. del Coz Diaz, F.Rodriguez Mazon, P.J. Garcia Nieto and F.J. Suarez Dominguez (2002); 'Design and finite element analysis of a wet cycle cement rotary kiln', Finite Elements in Analysis and Design, 39, 17-42
2. Gongfa Li, Ze Liu, Guozhang Jiang, Honghai Liu and Hegen Xiong (2015): 'Numerical simulation of the influence factors for rotary kiln in temperature field and stress field and the structure optimization', Advances in Mechanical Engineering, vol 7(6), 1-15
3. Jagendran Ravindran and Soundarajan Krishnan (2016): 'Studies on Thermal Analysis of Cement Rotary Kiln Based on Clinker Coating Materials on Refractories, Energy and Monetary Savings', International Congress on Recent Development in Engineering and Technology (RDET-16), Kuala Lumpur (Malaysia)
4. Susana Arad (2016): 'Thermal analysis of the rotary kiln through FEA', Recent Advances in Finite Differences and Applied & Computational Mathematics
5. Jia Xianzhao, Zhang Zhiwen and Liu Hongbin (2011): 'Finite element analysis of rotary kiln cylinder', Advanced Materials Research, Vols 228-229, pp174-178.

